Int J Adv Manuf Technol (2012) 59:1025–1035
DOI 10.1007/s00170-011-3566-1

ORIGINAL ARTICLE

Balling behavior of stainless steel and nickel powder during selective laser melting process

Ruidi Li · Jinhui Liu · Yusheng Shi · Li Wang · Wei Jiang

Received: 14 May 2011 / Accepted: 3 August 2011 / Published online: 18 August 2011

Abstract Balling phenomenon, as a typical selective laser melting (SLM) defect, is detrimental to the forming quality. In this work, a detailed investigation into the balling behavior of selective laser melting of stainless steel and pure nickel powder was conducted. It was found that the SLM balling phenomenon can be divided into two types generally: the ellipsoidal balls with dimension of about 500 μm and the spherical balls with dimension of about 10 μm. The former is caused by worsened wetting ability and detrimental to SLM quality; the latter has no obvious detriment to SLM quality. The oxygen content plays an important role in determining the balling initiation, which can be considerably lessened by decreasing the oxygen content of atmosphere to 0.1%. A high laser line energy density, which can be obtained by applying high laser power and low scan speed, could enable a well-wetting characteristic. The effect of scan interval on balling initiation is not obvious as long as the scan track is continuous. The surface remelting procedure can also alleviate the balling effect in a certain extent, due to the melting and wetting of metal balls. Moreover, the balling phenomenon of pure nickel was also studied, and the results implied that the balling discipline had a universality.

Keywords Selective laser melting · Balling behavior · Stainless steel · Nickel

R. Li (✉)
State Key Laboratory of Solidification Processing,
Northwestern Polytechnical University,
Xi'an 710072, People's Republic of China
e-mail: lrdcsu@gmail.com

J. Liu
Heilongjiang Institute of Science and Technology,
Harbin 150027, People's Republic of China

Y. Shi · L. Wang · W. Jiang
State Key Laboratory of Material Processing and Die & Mould Technology, Huazhong University of Science and Technology,
Wuhan 430074, People's Republic of China

1 Introduction

Selective laser melting (SLM), as a new and perspective method of rapid manufacturing, enables the fabrication of prototypes with complex shapes directly from metallic powder [1, 2]. SLM has aroused wide concerns and been widely used in aerospace, biomedicine, and many other engineering fields, offering a series of advantages compared with traditional processing techniques: high complexity, time saving, versatility, etc. [3–6]. However, during the SLM process, the laser molten track possesses a shrinking tendency to decrease the surface energy under the action of surface tension. Thus, the balling phenomenon is very easily formed during SLM process, which is detrimental to quality of SLM processed part and hinder the further development of SLM technology [7–9]. Detailedly, the disadvantageous effect of balling phenomenon to forming quality of SLM technology can be summarized as follows:

1. The balling phenomenon could increase the surface roughness; thus, the SLM component needs polishing treatment to be used. The post-processing procedures are not only trivial but also decrease the dimensional accuracy.
2. A large number of pores in SLM component tend to be formed between many discontinuous metallic balls [10], resulting in the poor mechanical property of SLM part.

3. When the severe balling phenomenon occurs, the bellied metal balls tend to hinder the movement of paving roller; thus, the unfinished part can be scratched by paving roller or the powder paving step is stopped immediately.

Although it is known that the balling phenomenon occurs with the decrease of free energy, the formation process, mechanism, and influencing factors are extremely complicated and not clear, due to the complex physical, chemical, and laser interaction [11, 12]. According to these problems, previous literatures have been issued on the scope of SLM balling phenomenon. Tolochko et al. studied the detailed balling process during the interaction between laser and metal powder [13]. The balls were classified as plate, cup, and sphere according to shape designation, and the respective formation mechanisms were also analyzed in their research. Gu et al. investigated the balling behavior of Cu-based and stainless steel under the action of CO_2 laser [7, 14, 15]. They pointed out that balls can be divided into two types: The first kind of ball formation was due to inadequate laser energy input with little liquid content, and the second kind of ball was owing to molten pool splashing under high scan speed. Kruth et al. analyzed the addition of deoxidizer into powder system to alleviate the balling level [8]. Simchi and Pohl researched the surface conditions of pure iron powder under different scan line spacings, pointing out that the balling was because of capillary instability and the balling can be lessened by reducing the scan line spacing [16]. Childs et al. studied the balling conditions of single laser track under different scan speeds and laser powers and established a process window describing the relationship between the processing parameters and melting track features, which can be used in selecting proper parameters and preventing balling [17].

However, the previous literatures have not studied the balling phenomenon comprehensively. First, the harmfulness of balling to SLM forming quality has not been analyzed detailedly. Second, the effect of oxygen content in atmosphere on the balling initiation has not been studied. Third, the effect of layer thickness on the balling initiation on a continuously sloped substrate has not been investigated. Fourth, the surface remelting on the balling has not been studied. Fifth, the universality of balling theory has not been tested by different powder. Moreover, since the SLM technology is carried out from line to surface and then from surface to body, a systematic study on the negative factor of balling and the balling behaviors of line, surface, body, remelting procedure, and material universality is also regarded necessary. In this study, the balling characteristics of SLM in line, surface, and body processes were investigated. The influences of processing conditions (oxygen content, scan speed, laser power, scan interval, layer thickness, surface remelting) on the balling initiation were studied using stainless steel as representative material, with the purpose of disclosing the basic laws of balling, and then the balling laws were verified to disclose its universality using nickel powder.

2 Experimental

In this study, gas atomized 316-L stainless steel powder and electrolytic nickel powder were used. The gas atomized stainless steel powder exhibited a spherical shape with an average particle size of 20 μm (Fig. 1a). The electrolytic nickel powder exhibited a dendritic shape with an average particle size of 30 μm (Fig. 1b). The powders were stored by vacuum packing to avoid oxidization.

The SLM experiment was conducted by self-developed commercial HRPM-IIA SLM machine, consisted mainly of a 200-W fiber laser (IPG Laser GmbH), a F-theta lens system, a powder layering apparatus, an inert gas protection system, an oxygen recorder, and a computer-control system. The maximal processing space of this machine was 250 (L)×250 (W)×250 mm (H).

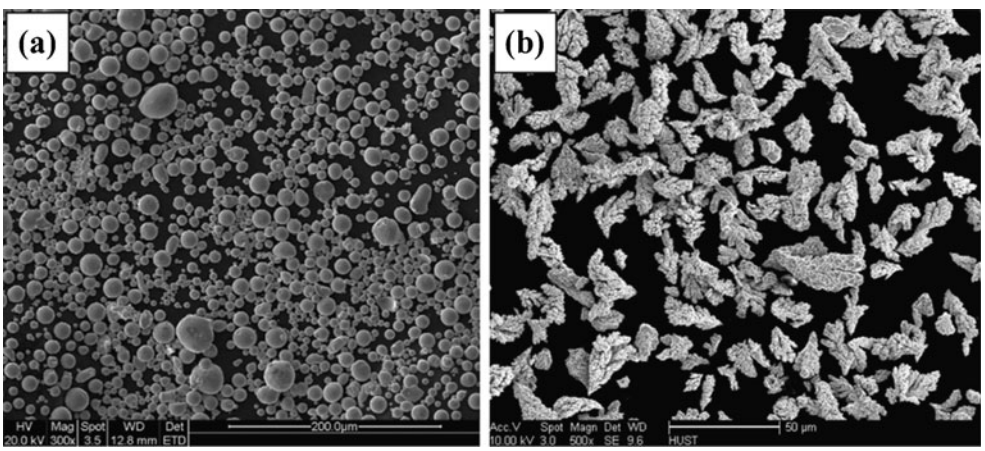

Fig. 1 SEM images showing characteristic morphologies of starting powders: **a** gas atomized 316L stainless steel; **b** electrolytic pure nickel

Before the SLM specimen was to be fabricated, a steel substrate was installed on the building platform and leveled. Then the building chamber was filled with argon gas with different contents to study the influence of oxygen contents on the balling effects. A thin powder layer with a certain thickness was paved on the steel substrate by a paving roller. Afterward, the laser beam scanned the powder layer to prepare lines, layers, and multi-layers specimens with different SLM parameters to research the influence the parameters on the balling effects. The SLM processing parameters were laser power (P) of 100–200 W, scan speed (v) of 50–800 mm/s, hatch spacing (h) of 0.1–0.8 mm, and layer thickness (d) of 0.05–0.5 mm.

At last, the surface morphologies and microstructure of as-prepared samples were by Quanta 200 scanning electron microscope (SEM). The chemical composition of SLM samples were obtained by energy dispersive X-ray spectrometer analysis.

3 Results and discussion

3.1 Balling characterization

Figure 2 illustrates surface morphologies of SLM specimen, which reflects the typical balling characteristics. In the low magnification, it can be seen that the processing surface is separated by a large number of big-sized metallic balls; thus, the surface is discontinuous, as is evidenced in Fig. 2a. In the high magnification of Fig. 2a, as shown in Fig. 2b, many small-sized metallic balls are detected. In general, the SLM balling effect can be divided into two types: (1) ellipsoidal balls: the size is about 500 μm; (2) spherical balls: the size is about 10 μm. The above balling classification could contribute to understand the balling mechanisms and obtain effective balling controlling method. Gu and Shen have also studied balling phenomenon during direct metal laser sintering process, and the two typical balling types with big-sized and small-sized scales were detected in their study [14]. However, the CO_2 laser used in their study is different from fiber laser in laser mode, balling size, and shape.

3.2 Negative factor of balling

Although the existence of small-sized balling is universal in SLM, it will not block the powder paving process; thus, the negative factor of small-sized balling can be ignored, while the big-sized balling can not only induce a coarse surface but also tends to block the powder paving process, leading to severe forming defects, which can be listed as follows: (1) The metal part can be fractured by severe friction between paving roller and balling; (2) the forming process could not be continued when high friction resistance occurred. To better illustrating the negative factor of balling, an example of balling caused defect, as shown in Fig. 3, is presented here.

According to our SLM experiment, the blocking effect induced by balling is depicted in Fig. 4, and the detailed processes are as follows:

1. First layer paving (Fig. 4a): A powder layer with the thickness of H is paved on the forming substrate.
2. Laser scanning of the first layer (Fig. 4b): Laser scanning induces the big-sized balling, which height exceeds the layer thickness H.
3. Second layer paving (Fig. 4c): Although the paving roller can constrainedly pass the top surface of balling, the roller fluctuates up and down during the powder paving process and yields an uneven powder layer which thickness exceeds $2H$.
4. Laser scanning of the second layer (Fig. 4d): A more serious balling effect is produced and its height outdistances the thickness of $3H$, leading to the serious roller jam during the next powder layer paving process; accordingly, the SLM forming process is broken down.

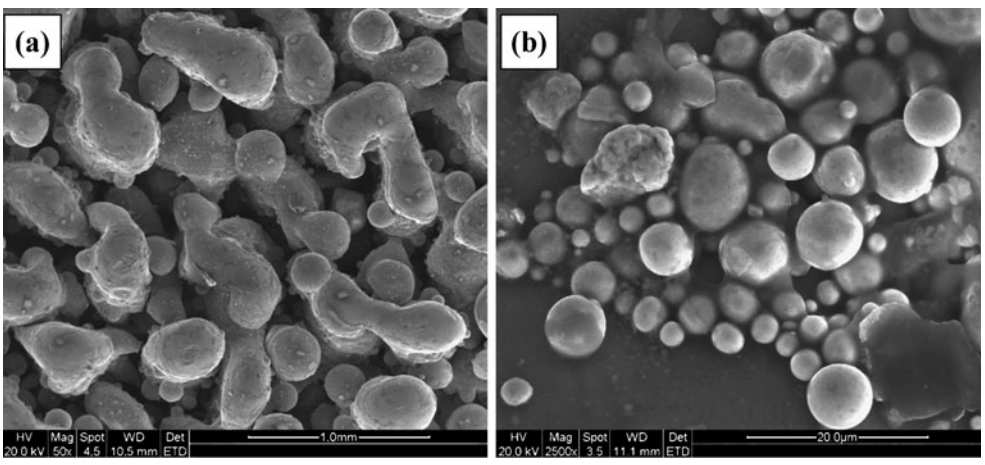

Fig. 2 SEM images showing typical balling phenomenons: **a** big-sized balls, 500 μm; **b** small-sized balls, 10 μm

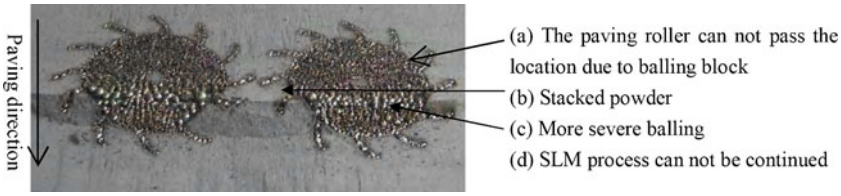

Fig. 3 An example of balling induced SLM forming defect

Therefore, the big-sized balling is a noteworthy defect, which hinders the advance of SLM technology seriously. Systematically investigate the balling mechanism and lessen the harm effect are vital for the advance of SLM technology. The following text will analyze the balling factors in detail.

3.3 Effects of SLM conditions on the balling initiation

In the SLM process, the balling phenomenon is very complicated. In one hand, the balling behavior contains balling dimension, shape, distribution, and density, which

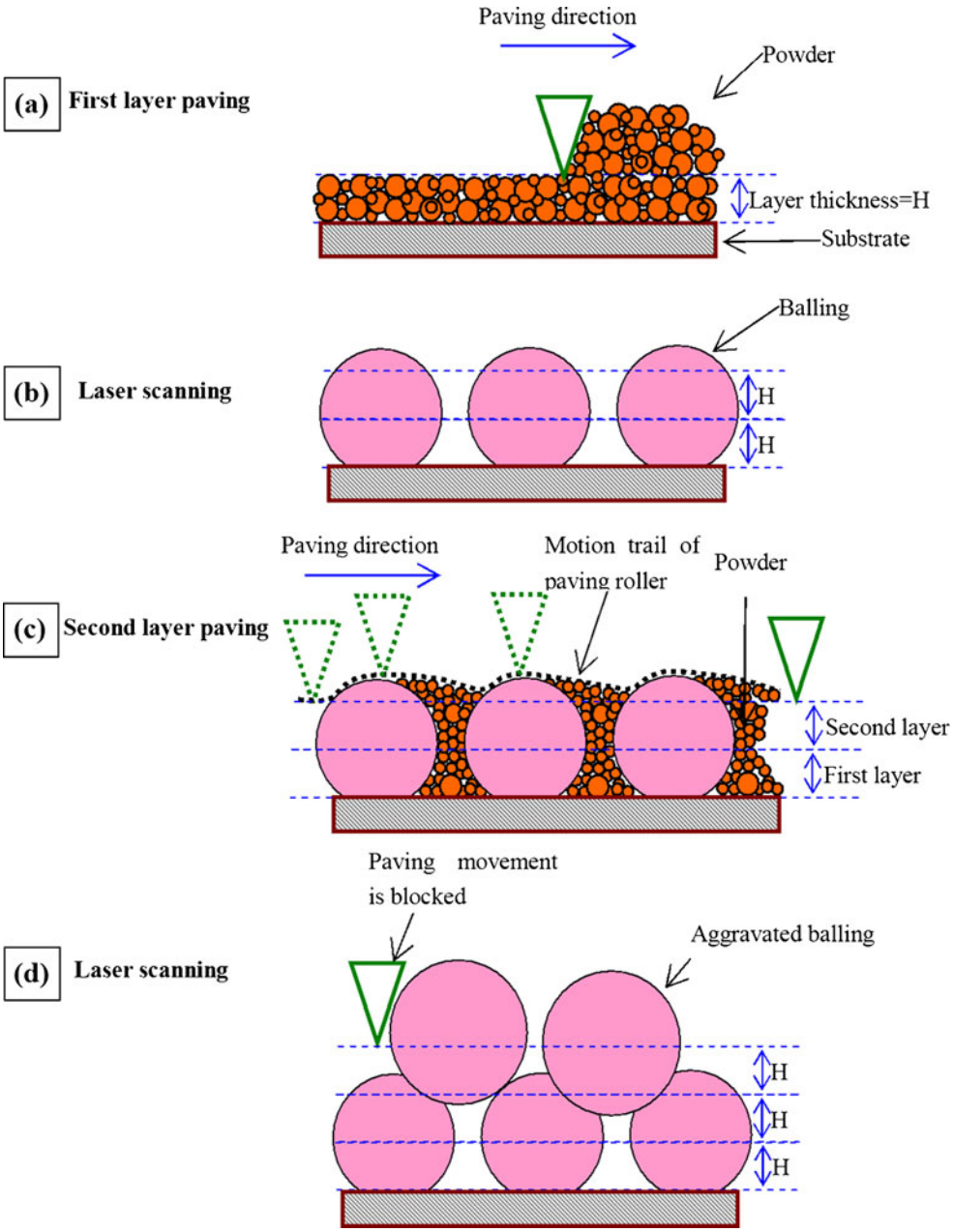

Fig. 4 Schematic diagram showing the balling induced block effect on the movement of paving roller: **a** paving of first powder layer; **b** balling initiation after laser scanning; **c** paving of second powder layer; **d** even severe balling initiation after laser scanning and the paving movement was blocked

are difficult to be characterized quantificationally. One the other hand, the influencing factors of balling behavior are complex owing to multi-mode heat, mass, and momentum transfer. When the laser scans the metal powder, the laser energy is absorbed by metal powder and the temperature is elevated immediately, yielding a molten pool. Then the molten pool tends to flow and wet the substrate, which is relevant to the viscosity of molten pool. Thus, the SLM parameters determine the temperature and accordingly the viscosity of molten pool, which govern the wetting ability and the balling behavior. Overall, it is very extremely difficult to characterize the balling phenomenon quantificationally. In this work, the influencing factors of balling phenomenon, such as oxygen content, laser power, scan speed, scan interval, layer thickness, and remelting procedure, were studied qualitatively.

3.3.1 Oxygen content

Figure 5 illustrates the influence of oxygen content on the balling characteristic. The scan speed of 50 mm/s, laser power of 190 W, scan interval of 0.2 mm, and layer thickness of 0.05 mm were fixed as constants. It can be seen that the oxygen content in atmosphere plays a crucial effect on the balling characteristics. At a relative low oxygen content of 0.1%, the morphologies of as-received scan tracks were clear and overlapped in a favorable condition, yielding a flat surface without big-sized balling except a small number of small-sized balling (Fig. 5a). When the oxygen content was increased to 1%, the scan tracks became indistinct, coupled with the generation of visible big-sized balling. At a more higher oxygen content of 10%, the scan tracks became discontinuous, accompanied with serious balling phenomenon and deteriorative surface condition. It was reasonable to conclude that oxygen in atmosphere has a pronounced effect on ball formation, due to the oxidation of molten pool and accordingly worsened wetting characteristic with oxide at the wetting interface. In order to support this conclusion, EDS test was performed to detect the oxygen content in as-prepared SLM sample, as illustrated in Table 1. It was found that with increasing the oxygen content in atmosphere from 0.1% to 10%, the oxygen content in SLM sample was

Table 1 Relationship between oxygen content in SLM sample and oxygen content in atmosphere

Oxygen content in atmosphere (%)	0.1	2	10
Oxygen content in SLM sample (wt.%)	2.11	5.81	7.69

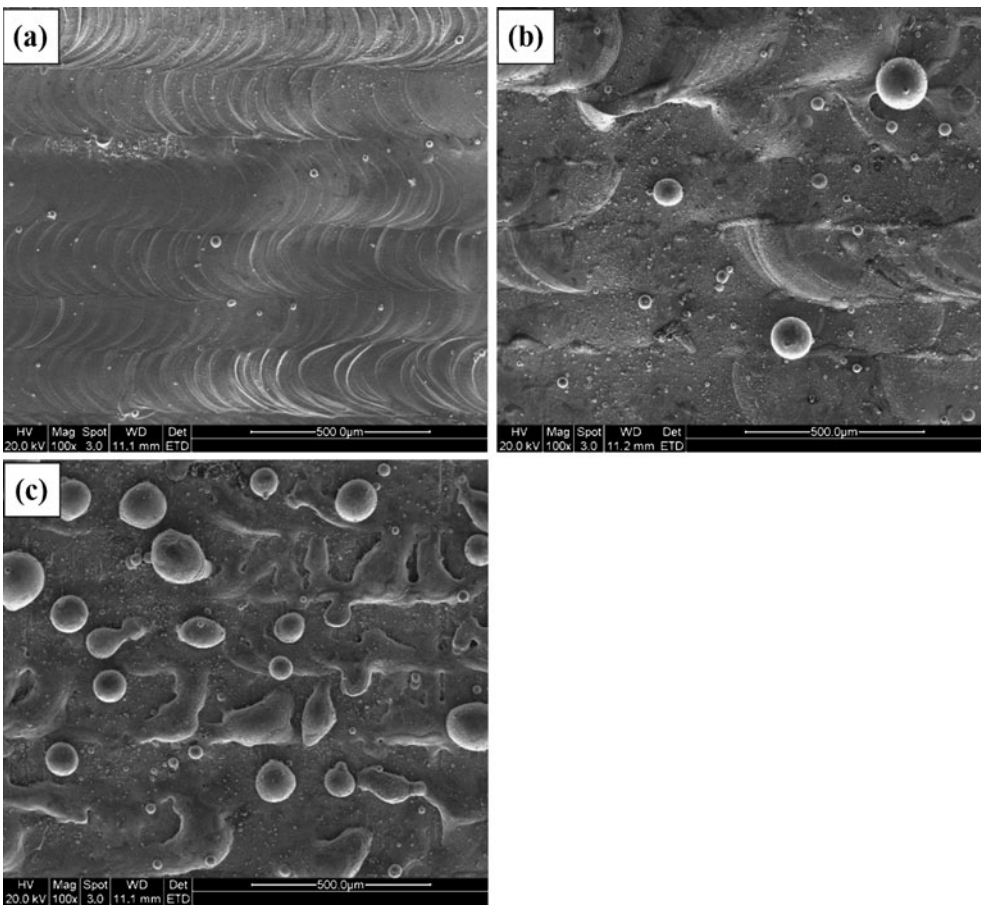

Fig. 5 SEM image showing the balling characteristics under different oxygen contents in atmosphere: **a** 0.1%; **b** 2%; **c** 10%

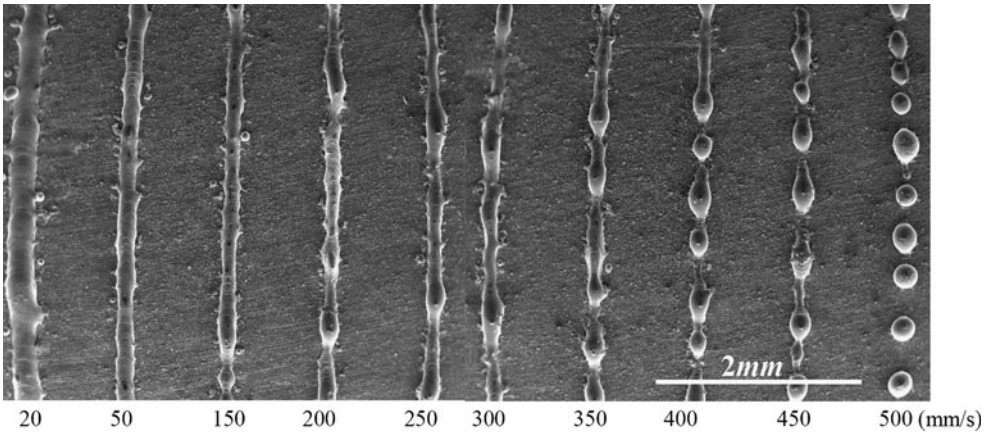

Fig. 6 SEM images showing the balling characteristics of single scan tracks under different scan speeds

also increased from 2.11% to 7.69%, respectively. Therefore, the oxygen plays an important role in inducing the balling initiation, which can be restrained by decreasing the oxygen content in atmosphere.

3.3.2 Scan speed

Figure 6 depicts the balling characteristics of single scan tracks under different scan speeds. The laser power of 190 W was fixed as constant. It was visible that on increasing the scan speeds, the scan track widths were narrowed gradually. In the meanwhile, the scan tracks became discontinuous and broke up into balling. It was because the laser energy was low under high scan speed [18], leading to worsened wetting ability and accordingly balling initiation. In addition, under high scan speed and low laser energy, the as-formed molten pool dimension was too small that the contact area between molten pool and substrate was considerably limited, leading to unfavorable wetting, flowing, spreading characteristics, and corresponding balling phenomenon.

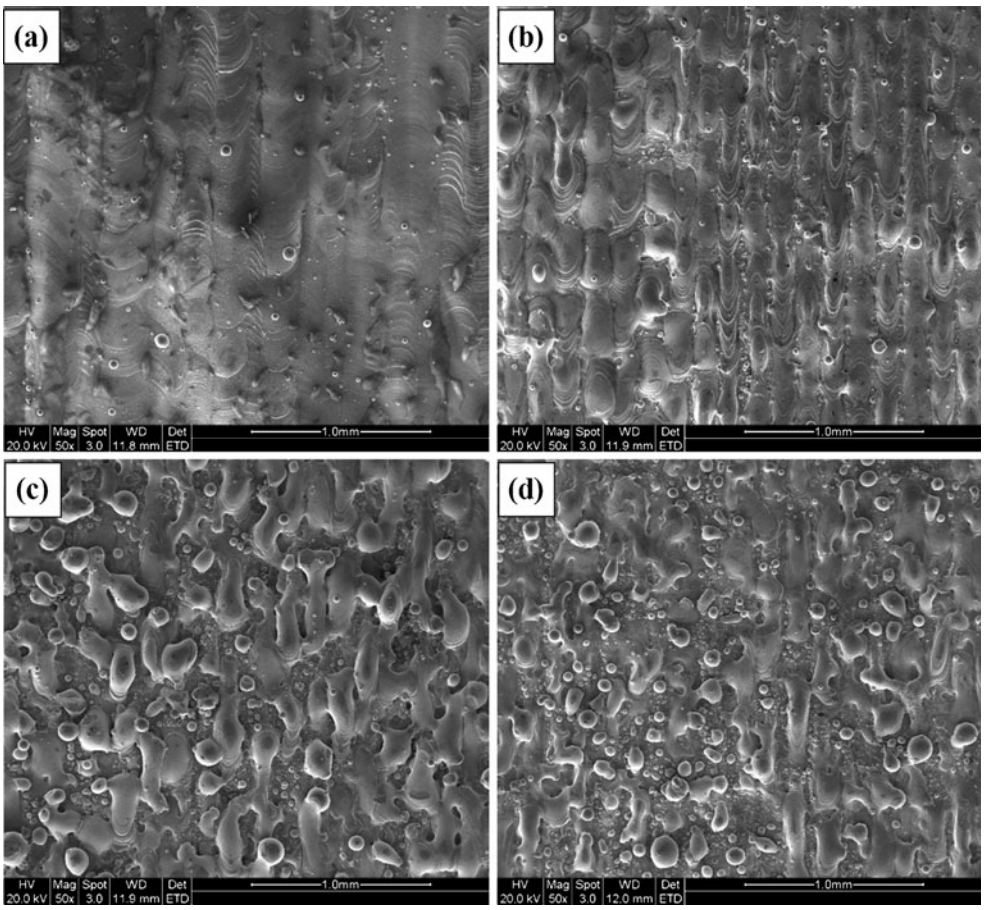

Fig. 7 SEM images showing the balling characteristics of SLM layers under different scan speeds: **a** 50 mm/s; **b** 400 mm/s; **c** 600 mm/s; **d** 800 mm/s

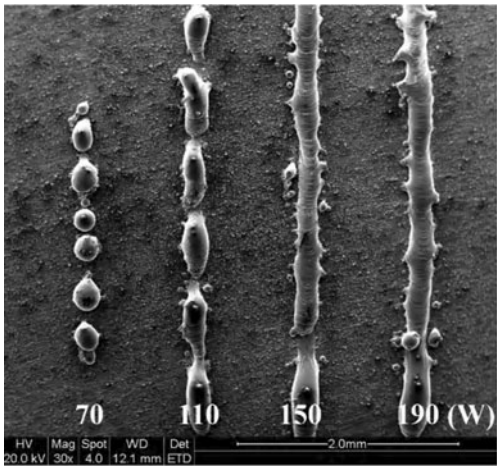

Fig. 8 SEM images showing the balling characteristics of single scan tracks under different laser powers

The balling conditions of single SLM layer were characterized, as shown in Fig. 7. The laser power of 190 W and scan interval of 0.15 mm were constants. At a lower scan speed of 50 mm/s, the scan tracks were continuous and overlapped in a well condition, giving rise to a smooth surface without visible big-sized balling. On increasing the scan speed to 400 mm/s, the scan tracks were inclined to discontinuous, thereby a relative coarse surface. When a much higher scan speed of 600 mm/s was applied, the as-received surface exhibited a very coarse surface with many metal balls. Similarly, with the further increase of scan speed to 800 mm/s, the balling effect was intensified sequentially, while the ball size was reduced compared with that at scan speed of 400 and 600 mm/s. Consequently, it can be inferred that no matter the single track scanning and the single layer scanning process, the high scan speed militate against the continuity of scan tracks and the wetting ability of molten pool, tending to incurring the occurrence of balling phenomenon.

3.3.3 Laser power

Figure 8 elucidates the balling characteristics of single scan tracks at different laser powers. The scan speed was fixed as 200 mm/s. It showed that the balling characteristics are also strongly influenced by laser powers. At lower laser power of 70–100 W, the scan tracks were discontinuous combined with the balling initiation. On increasing the laser power to 150–190 W, the scan tracks became continuous without presence of any balling initiation. Therefore, the high laser power can provide enough input energy, favoring the wetting and spreading of molten pool, which was similar to the influence of scan speed on balling initiation.

3.3.4 Scan interval

According to the morphologies of scan tracks produced at different scan speeds and laser powers (Figs. 7 and 8), it

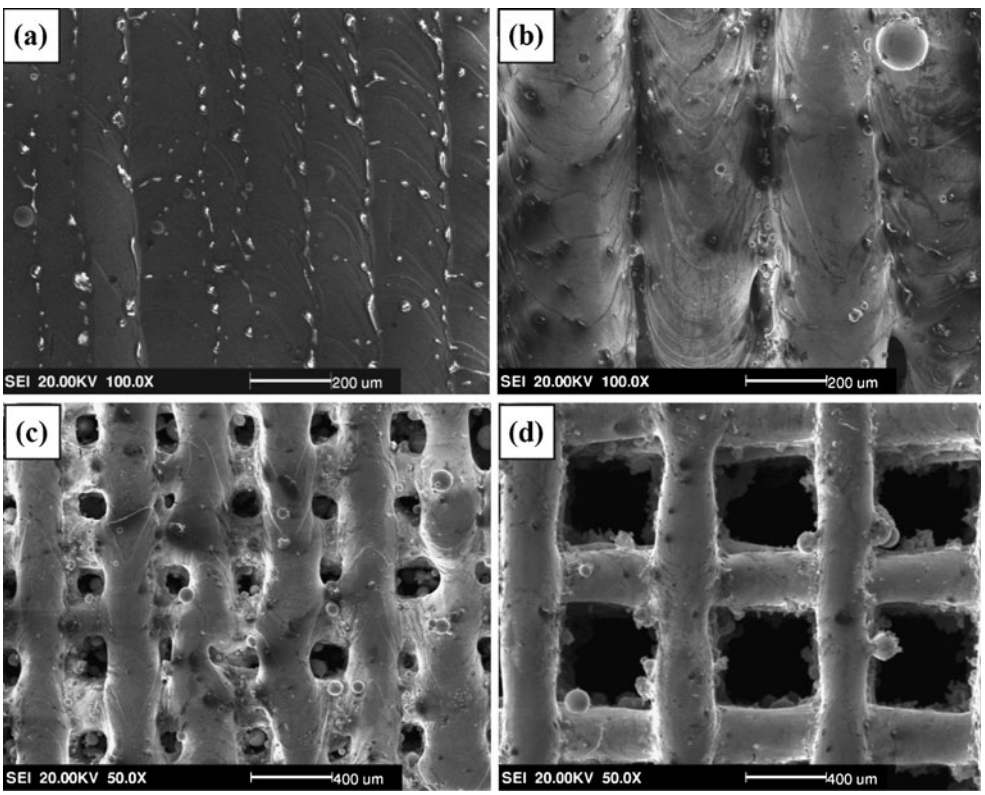

Fig. 9 SEM images showing the balling characteristics of SLM layers under different scan speeds: **a** 0.15 mm; **b** 0.3 mm; **c** 0.4 mm; **d** 0.8 mm

Fig. 10 Schematic diagram showing the sloped substrate

can be found that the scan track was continuous without balling under laser power of 190 W and scan speed of 100 mm/s. Figure 9 shows the surface morphologies at different scan intervals with the laser power of 190 W and scan speed of 100 mm/s as constants. At a narrow scan interval of 0.15 mm, the scan tracks were overlapped tightly, inducing a fully dense and comparatively smooth surface (Fig. 9a). As scan interval increased to 0.3 mm, the scan tracks were continuous and the as-produced surface was also dense and smooth although the lap rate was decreased. With the further increase of scan interval to 0.4 mm, many regular pores were formed, which were separated by continuous scan tracks. Similarly, when the scan interval was further increased to 0.8 mm, the as-produced pores were enlarged. Overall, it can be inferred that there is no big-sized balling no matter the scan tracks can be overlapped or not, as long as the scan track is continuous.

3.3.5 Layer thickness

In order to investigate the influence of layer thickness on the balling characteristics of SLM process, the single track and SLM bulk material were prepared with different layer thicknesses. A sloped steel substrate was manufactured, which can produce a gradient layer thickness, as schematically shown in Fig. 10. Then the single scan line experiment was conducted on this sloped substrate to disclose the effect of layer thickness on the balling. The laser power of 190 W and scan speed of 50 mm/s were fixed as constants. It was noticeable that the layer thickness has a pronounced effect on balling initiation, as clearly indicated in Fig. 11. At the AB zone (Fig. 11a), all the scan tracks were continuous and possessed similar morphologies (Fig. 11b), due to the identical layer thickness and accordingly the same wetting characteristics. While at the BC zone (Fig. 11a), the layer thickness was increased gradually from left to right, thus incurring the occurrence of balling phenomenon gradually (Fig. 11c). Moreover, it can also be seen that the scan track was widened with the increase of layer thickness owing to the more powder volume. Consequently, the thin powder layer is favorable for the continuity of scan track.

Then the effect of layer thickness on the balling characteristics of SLM bulk material was investigated, as shown in Fig. 12. The laser power of 190 W, scan speed of 100 mm/s, and scan interval of 0.15 mm were fixed as

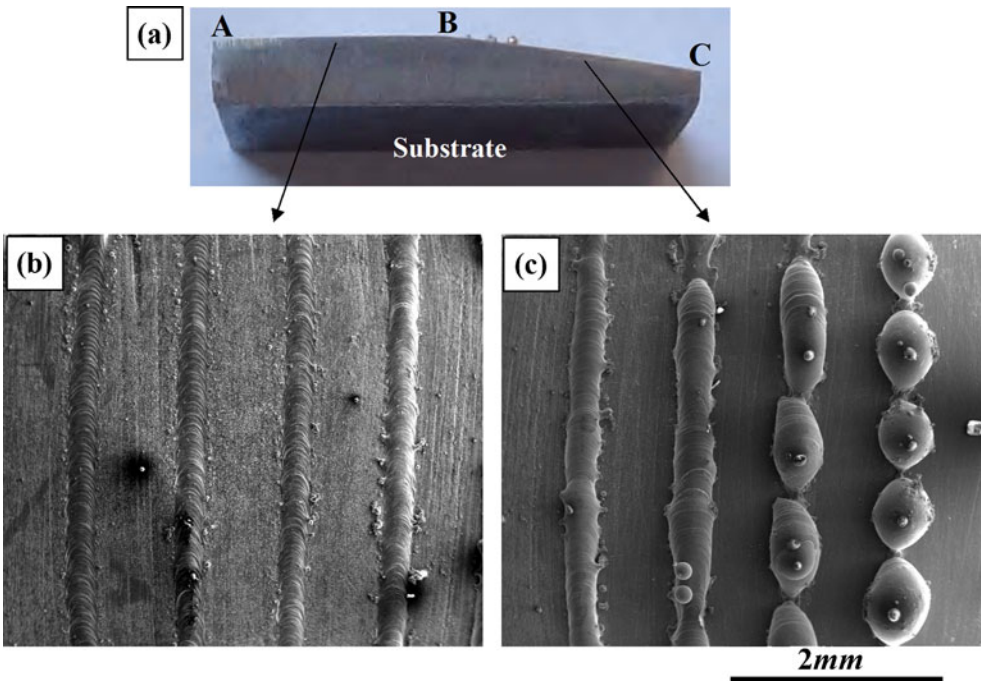

Fig. 11 Effect of layer thickness on the balling characteristics of scan tracks

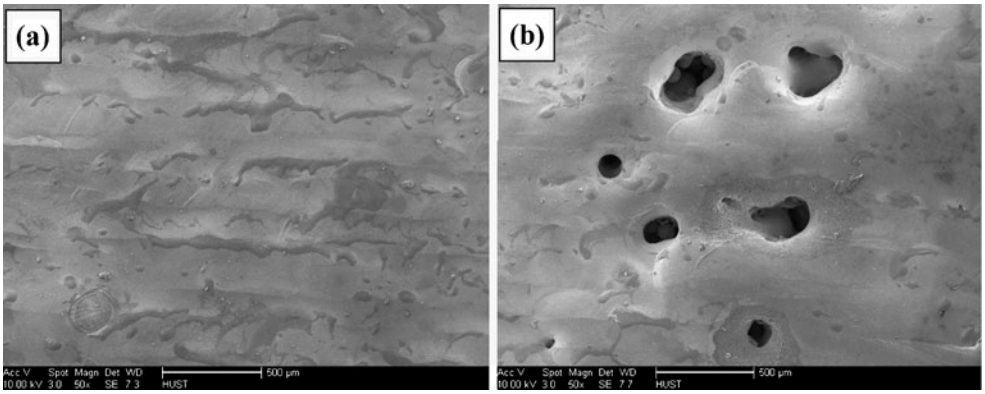

Fig. 12 SEM images showing the surface conditions of bulk materials fabricated with different layer thickness: **a** 0.05 mm; **b** 0.1 mm

constants. At a thinner layer thickness of 0.05 mm, the as-prepared surface possessed a smooth characteristic, exhibiting a well-wetting ability. However, at a thicker layer thickness of 0.1 mm, several agglomerates and pores were present on as-prepared surface, which indicated the worsened wetting ability.

Therefore, the thicker layer thickness is unfavorable for the wetting ability of molten pool regardless of the single track or the multi-layers process. The above results can be explained as follows. Firstly, at a thicker thickness, the layer energy absorbed in unit volume of powder is insufficient; hence, the temperature of molten pool is low, resulting in a weak flow ability and balling phenomenon. Secondly, although a thicker layer thickness could enable a big molten pool, the molten pool is far away from the substrate, leading to a relatively small contact area between molten pool and substrate, as schematically illustrated in Fig 13. In this condition, the small wetting area could not support a big molten pool, thereby the molten track tends to break up into balls.

The above balling discipline was established based on 316L stainless steel. However, whether the above balling discipline was appropriate for the other metal powder was still not clear. In order to disclose this, the pure nickel powder was selected as representative material (Fig. 1b) for laser scanning experiment to investigate its balling behavior. The experiment of single track scanning of pure nickel material was also performed on the sloped steel substrate (Fig. 10a). The laser power of 190 W and scan speed of 50 mm/s were fixed as constants. Figure 14 shows the morphologies of single tracks under varied layer thickness. It also can be seen that the increased layer thickness could enable the balling initiation gradually, which was similar to that of 316L stainless steel powder. Furthermore, when the single track scanning was conducted at a thicker thickness, one can noticed that there were many pores present in the scan tracks (Fig. 14b–d), which was appreciably different from the scan tracks obtained at a thinner layer thickness (Fig. 14a), despite the mechanism of pore formation in scan track was not clear. In general, the above results reveal that the balling initiation has a universality in a certain extent.

3.3.6 Surface remelting

Two SLM samples were prepared by once and twice scanning in each layer manufacturing process, respectively, for the purpose of understanding the effect of remelting procedure on the balling phenomenon, as shown in Fig. 15. The other parameters were fixed as constants. When the SLM sample was fabricated without remelting, several metal balls were present in the surface morphology, although the scan tracks were continuous and overlapped in good quality (Fig. 15a). Interestingly, when the remelting technique was applied in SLM process, a relatively smooth surface was obtained without present of any metal balls (Fig. 15b). Thus, it is reasonable to conclude that the remelting procedure is in capable of the melting of the metal balls, which is then converted to molten pool and wet the surface favorably with the disappearance of balling phenomenon.

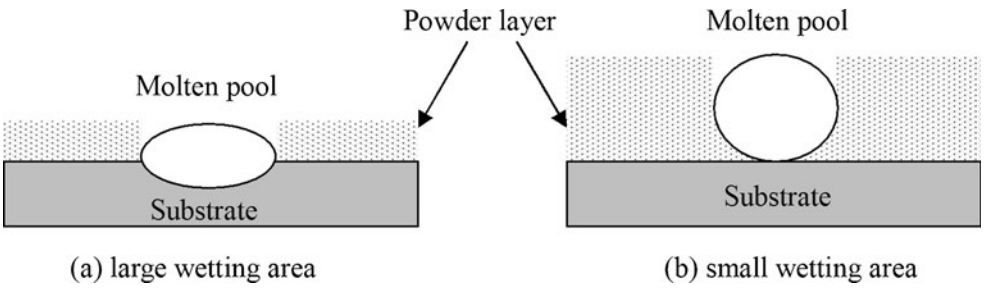

Fig. 13 Schematic diagram showing the effect of layer thickness on the wetting condition

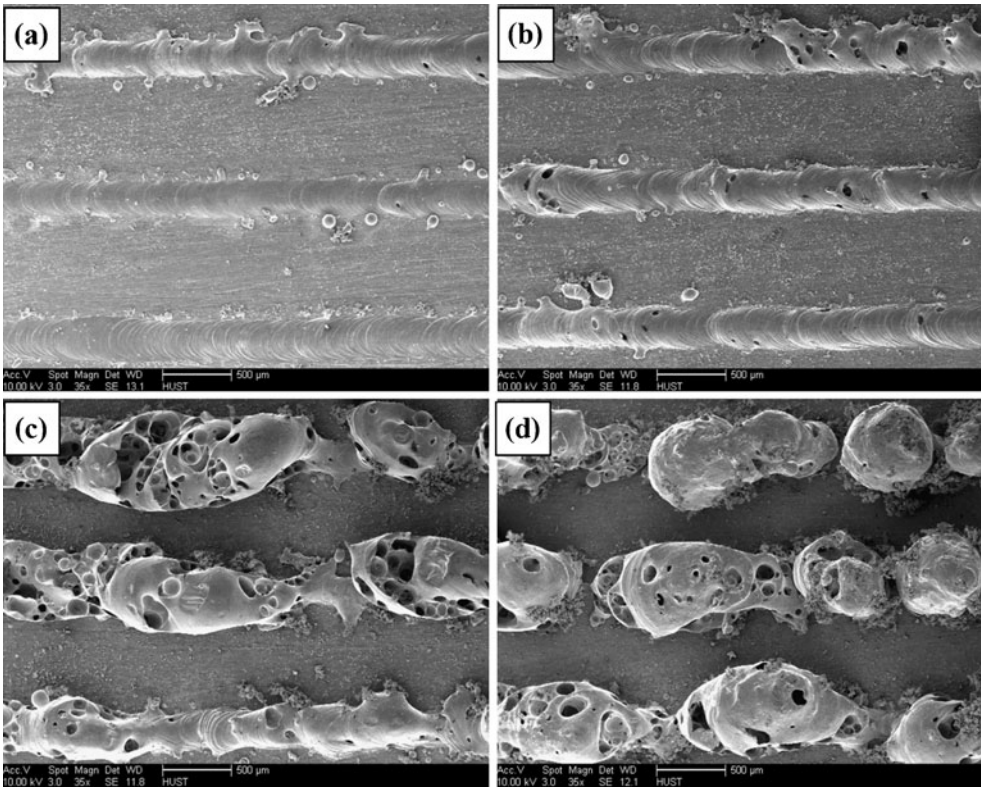

Fig. 14 SEM images showing the effect of layer thickness on the balling characteristics of scan tracks: The layer thickness was increased gradually from **a** to **d**

4 Conclusion

A detailed study has been performed to study the balling behavior of stainless steel and pure nickel powder in SLM process. The following conclusions can be drawn:

1. The SLM balling can be divided into two types: ellipsoidal balls, which is caused by worsened wetting ability and detrimental to SLM forming quality with dimension of about 500 μm, and spherical balls, which has no obvious detriment to SLM quality with dimension of about 10 μm.
2. The balling phenomenon can be restrained by decreasing the oxygen content in atmosphere. SLM at oxygen content of 0.1% could produce a smooth melting surface without balling initiation. While at a higher oxygen content of 2% and 10%, the balling phenomenon tends to generate.
3. At a high laser line energy density (high laser power and low scan speed), the as-prepared molten track possesses a beneficial continuity without balling phenomenon, due to the well-wetting characteristic.
4. The scan interval has no obvious effect on the balling phenomenon. As long as the scan track is continuous, there is no big-sized balling no matter the scan tracks can be overlapped or not.
5. The balling phenomenon can also be alleviated in a certain extent by remelting of SLM surface, through which the metal balls could be melted and then wet the surface favorably.

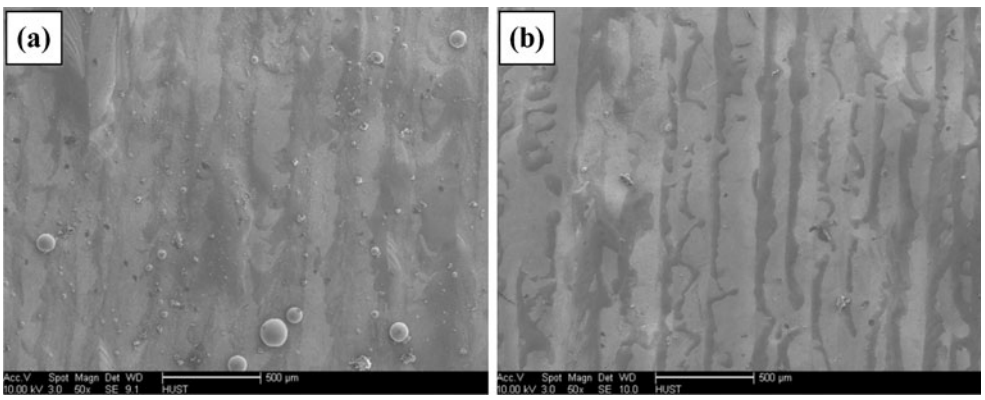

Fig. 15 SEM images showing the balling characteristics at different scanning strategy: **a** without remelting; **b** remelting

6. The single track scanning test on the sloped substrate of pure nickel powder showed that the increased layer thickness could enable the balling initiation gradually, which was similar to that of 316L stainless steel powder, indicating the balling discipline had a universality.

Acknowledgments The authors would like to acknowledge the China Postdoctoral Science Foundation (20110491684) and the Natural Science Foundation of China (61078078).

References

1. Tolosa I, Garciandia F, Zubiri F, Zapirain F, Esnaola A (2010) Study of mechanical properties of AISI 316 stainless steel processed by "selective laser melting", following different manufacturing strategies. Int J Adv Manuf Technol 51(5–8):639–647
2. Zhang WX, Shi YS, Liu B, Xu L, Jiang W (2009) Consecutive subsector scan mode with adjustable scan lengths for selective laser melting technology. Int J Adv Manuf Technol 41(7–8):706–713
3. Yadroitsev I, Bertrand P, Smurov I (2007) Parametric analysis of the selective laser melting process. Appl Surf Sci 253(19):8064–8069
4. Li RD, Shi YS, Liu JH, Xie Z, Wang ZG (2010) Selective laser melting W-10 wt.% Cu composite powders. Int J Adv Manuf Technol 48(5–8):597–605
5. Jhabvala J, Boillat E, André C, Glardon R (2011) An innovative method to build support structures with a pulsed laser in the selective laser melting process. Int J Adv Manuf Technol. doi:10.1007/s00170-011-3470-8
6. Wang FD (2011) Mechanical property study on rapid additive layer manufacture Hastelloy® X alloy by selective laser melting technology. Int J Adv Manuf Technol. doi:10.1007/s00170-011-3423-2
7. Gu DD, Shen YF (2007) Balling phenomena during direct laser sintering of multi-component Cu-based metal powder. J Alloy Compd 432(1–2):163–166
8. Kruth JP, Froyen L, Van Vaerenbergh J, Mercelis P, Rombouts M, Lauwers B (2004) Selective laser melting of iron-based powder. J Mater Process Technol 149(1–3):616–622
9. Niu HJ, Chang ITH (1999) Instability of scan tracks of selective laser sintering of high speed steel powder. Scripta Mater 41 (11):1229–1234
10. Li RD, Shi YS, Wang ZG, Wang L, Liu JH, Jiang W (2010) Densification behavior of gas and water atomized 316L stainless steel powder during selective laser melting. Appl Surf Sci 256 (13):4350–4356
11. Simchi A (2006) Direct laser sintering of metal powders: mechanism, kinetics and microstructural features. Mater Sci Eng A 428(1–2):148–158
12. Simchi A, Petzoldt F, Pohl H (2001) Direct metal laser sintering: material considerations and mechanisms of particle bonding. Int J Powder Metall 37(2):49–61
13. Tolochko NK, Mozzharov SE, Yadroitsev IA, Laoui T, Froyen L, Titov VI, Ignatiev MB (2004) Balling processes during selective laser treatment of powders. Rapid Prototyping J 10(2):78–87
14. Gu DD, Shen YF (2009) Balling phenomena in direct laser sintering of stainless steel powder: metallurgical mechanisms and control methods. Mater Design 30(8):2903–2910
15. Gu DD, Shen YF, Yang JL, Wang Y (2006) Effects of processing parameters on direct laser sintering of multicomponent Cu based metal powder. Mater Sci Technol 22(12):1449–1455
16. Simchi A, Pohl H (2003) Effects of laser sintering processing parameters on the microstructure and densification of iron powder. Mater Sci Eng A 359(1–2):119–128
17. Childs THC, Hauser C, Badrossamay M (2004) Mapping and modelling single scan track formation in direct metal selective laser melting. Cirp Ann-Manuf Technol 53(1):191–194
18. Li RD, Shi YS, Liu JH, Yao HS, Zhang WX (2009) Effects of processing parameters on the temperature field of selective laser melting metal powder. Powder Metall Met Ceram 48(3–4):186–195